



## Adsorption of Pb(II) from aqueous solution using alkaline-treated natural zeolite: Process optimization analysis



N.A.S. El-Arish<sup>a</sup>, R.S.R. Mohd Zaki<sup>a</sup>, S.N. Miskan<sup>a</sup>, H.D. Setiabudi<sup>a,b,\*</sup>, N.F. Jaafar<sup>c</sup>

<sup>a</sup> Faculty of Chemical and Process Engineering Technology, College of Engineering Technology, Universiti Malaysia Pahang, Lebuhraya Tun Razak, 26300 Gambang, Kuantan, Pahang, Malaysia

<sup>b</sup> Centre for Research in Advanced Fluid & Processes, Universiti Malaysia Pahang, Lebuhraya Tun Razak, 26300 Gambang, Kuantan, Pahang, Malaysia

<sup>c</sup> School of Chemical Sciences, Universiti Sains Malaysia, 11800 USM Penang, Penang, Malaysia

### ARTICLE INFO

#### Keywords:

Optimization

Adsorption

Pb(II)

Alkaline-treated natural zeolite

### ABSTRACT

Alkaline-treated natural zeolite was prepared by sodium hydroxide treatment of natural zeolite and applied in the adsorption of Pb(II). The response surface methodology (RSM) analysis was conducted under manipulated variables of initial concentration ( $X_1 = 50\text{--}400$  mg/L), pH ( $X_2 = 2\text{--}10$ ), and adsorbent dosage ( $X_3 = 0.5\text{--}5.0$  g/L). The optimal condition was attained at  $X_1 = 240$  mg/L,  $X_2 = 6$ , and  $X_3 = 1.07$  g/L, with Pb(II) removal of 60.75%. The characterization of alkaline-treated natural zeolite of fresh and spent confirmed the adsorption of Pb(II) onto alkaline-treated natural zeolite. The reusability and regeneration experiments revealed the ability of the alkaline-treated natural zeolite in multiple cycles of the adsorption process. This study proved that alkaline-treated natural zeolite could be an alternative low-cost adsorbent for wastewater treatment containing Pb(II).

### Introduction

Heavy metal contamination is a severe issue for developing countries due to the presence of these elements in water effluents from multiple industries, including textiles companies, lead-acid batteries, papermaking, biomedical, mining, paints, and agriculture (Vardhan et al., 2019). Lead (Pb(II)) is one of the most toxic elements and has damaging consequences on human health, even at deficient levels (Shang et al., 2018). Besides, without realizing it, Pb(II) can be consumed through food and water. Therefore, the Environmental Quality (Industrial Effluents) Regulations 2009 has documented that the approved conditions before discharging industrial effluent of Pb(II) following standard A is 0.10 mg/L, meanwhile, standard B is 0.5 mg/L (Vardhan et al., 2019).

Numerous processes have been explored for removing dissolved Pb (II), including adsorption (Hasan and Setiabudi, 2019; Hasan et al., 2019), precipitation (Wu et al., 2021), photocatalytic degradation (Shang et al., 2018), flocculation & coagulation (Hargreaves et al., 2018), electro dialysis (Skibsted et al., 2018), and ultrafiltration (Roy Choudhury et al., 2019). Among them, the removal of Pb(II) using adsorption was known for its efficiency and economical, which has been utilized extensively in the purification of wastewater, industrial

discharge, and water supplies (Hasan and Setiabudi, 2019). It was also a favored approach for water purification since it can be operated in various conditions, is low cost, require low energy, does not produce any toxic by-product, and is flexible (Hasan et al., 2019).

Over the last few years, the utilization of low-cost alternative materials as viable adsorbents, including aquatic plants (Ohlbaum et al., 2018), wood materials (Yang et al., 2020), and agricultural by-products (Hasan et al., 2019) has attracted much attention for Pb(II) removal. However, these cost-effective adsorbents have a drawback by increasing water's chemical oxygen demand (COD) during adsorption (GilPavas et al., 2020). Therefore, it is vital to produce affordable and widely accessible adsorbents, such as the vast and non-toxic natural zeolite (Morante-Carballo et al., 2021). In addition, zeolites have been used in the application of molecular sieve, adsorption, and catalytic due to their structural features and desirable characteristic, including their thermostability, non-swelling, excellent chemical stability, reusability, regeneration, and high sorption equilibrium rate (Inglezakis et al., 2018; Din et al., 2021). However, their small pores impose diffusion limitations and restrict the access of reactant molecules to the active sites (Wu et al., 2012). Therefore, several treatment methods have been explored for zeolite modification, including the desilication method owing to its simplicity and feasibility. Interest-

\* Corresponding author at: Faculty of Chemical and Process Engineering Technology, College of Engineering Technology, Universiti Malaysia Pahang, Lebuhraya Tun Razak, 26300 Gambang, Kuantan, Pahang, Malaysia.

E-mail address: [herma@ump.edu.my](mailto:herma@ump.edu.my) (H.D. Setiabudi).

<https://doi.org/10.1016/j.totert.2022.100015>

Received 20 July 2022; Revised 8 October 2022; Accepted 11 October 2022

ingly, the desilication of zeolite with an alkaline solution is able to improve the porosity of zeolites through selective extraction of silicon atoms from the framework without a distinct change in the acidity and crystallinity (Wu et al., 2012).

However, there is a lack of study on the influence of the adsorbent's treatment and the optimization study of Pb(II) adsorption over alkaline-treated natural zeolite adsorbent. Consequently, this study intended to explore the effect of alkali treatment on the physicochemical properties of natural zeolite at different NaOH loading (0 g/L – 1.0 g/L) and their adsorption performance. Additionally, optimization analysis of Pb(II) adsorption using alkaline-treated natural zeolite at optimum conditions was also examined.

## Methodology

### Preparation of adsorbent

Natural zeolite originated from Indonesia and consisted of silicon oxide (SiO<sub>2</sub>) (59 %), aluminum oxide (Al<sub>2</sub>O<sub>3</sub>) (18 %), and a minor quantity of other oxide elements was used in this study. Alkaline-treated natural zeolite was synthesized following the method reported by Ates (Ates, 2018). First, the 20 g natural zeolite was combined with 250 mL of sodium hydroxide (NaOH, Merck) at 90°C with a mixing rate of 500 rpm. After 1 h, the solution was filtered, followed by washing with distilled water and drying in the oven (120°C, overnight). Next, the dried modified natural zeolite needs to undergo preliminary adsorption to determine an ideal alkaline-treated natural zeolite before proceeding with batch adsorption. The natural zeolite was treated with NaOH ranging from 0.5 to 5.0 g/L while maintaining other parameters to study the effects of NaOH loadings.

### Characterization

The functional groups of the alkaline-treated natural zeolite were analyzed using Fourier transform infrared (FTIR, Nicolet iS5) using the Attenuated total reflectance (ATR) approach. The morphology of the alkaline-treated natural zeolite was characterized using scanning electron microscopy (SEM, Hitachi S-4700). In addition, the elemental composition of alkaline-treated natural zeolite before and after adsorption was assessed using Energy Dispersive X-ray (EDX). The surface area and pore volume were measured using a Quantachrome Autosorb-1 analyzer.

### Batch adsorption and optimization experiment

The adsorption experiments were conducted according to the method described in the literature (Hasan and Setiabudi, 2019; Teong et al., 2019) at room temperature (27 °C). In brief, Pb(II) solution was prepared by mixing lead nitrate (Pb(NO<sub>3</sub>)<sub>2</sub>, 99 %, Sigma Aldrich) in deionized water. 0.5 g/L of alkaline-treated natural zeolite was added to 250 mL of Pb(II) solution under the constant speed of stirring. The pH of the Pb(II) solution was altered by hydrochloric acid (HCl, Merck) or NaOH (Merck). The samples were collected at a specific time interval before being centrifuged at 8000 rpm for 5 min. The absorbance of Pb(II) solution was assessed using UV–vis spectroscopy at 520 nm using dithizone (Merck) as a reagent. Equations (1) and (2) were applied to compute the amount of Pb(II) adsorbed, and the percentage of Pb(II) eliminated.

$$q_t = \left( \frac{C_o - C_t}{m} \right) \times V \quad (1)$$

$$\text{Removal (\%)} = \left( \frac{C_o - C_t}{C_o} \right) \times 100 \quad (2)$$

where  $q_t$  (mg/g) implies the quantity of Pb(II) adsorbed at a specific time.  $C_o$  (mg/L) and  $C_t$  (mg/L) indicate the Pb(II) concentration at ini-

tial and specific time.  $V$  (L) represents the volume of the Pb(II) solution, and  $m$  (g) indicates the dosage of alkaline-treated natural zeolite.

### Experimental design and optimization

Response Surface Methodology (RSM) (Statsoft Statistica 8.0) with a central composite design (CCD) was chosen. The manipulated variables were the initial concentration,  $X_1$  (50 mg/L–400 mg/L), pH,  $X_2$  (2–10), and adsorbent dosage,  $X_3$  (0.5 g/L–5.0 g/L). These independent variables were selected according to the findings obtained from the one-factor-at-a-time method (OFAT). A total of 16 different trials were carried out in triplicate. The outcomes were evaluated using the coefficient of determination ( $R^2$ ), analysis of variance (ANOVA), and 3D response surface plots.

### Regeneration and reusability

The regeneration and reusability studies were conducted according to the method described by Teong et al. (Teong et al., 2019). In brief, the reusability experiments were carried out at optimum RSM conditions with three adsorption cycles. After each cycle, the alkaline-treated natural zeolite was regenerated by shaking in phosphoric acid (0.1 M, Merck) for 1 h, washed with distilled water several times, and dried in the oven (120°C, overnight).

## Results and discussions

### Effects of NaOH loadings

Fig. 1 comprises the adsorption performance of six samples of alkaline-treated natural zeolite with different NaOH concentrations. The performance of alkaline-treated natural zeolite increased with

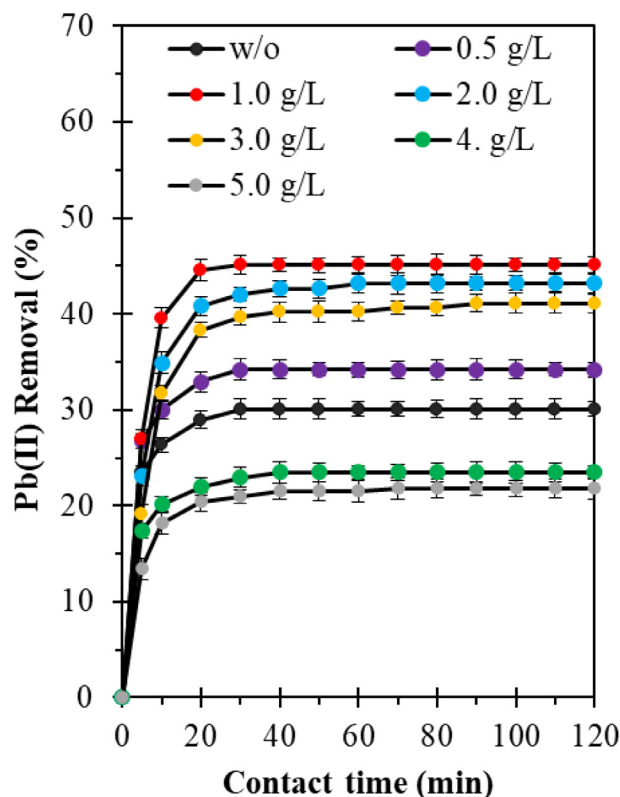


Fig. 1. Adsorption performance of natural zeolite without (w/o) and treated with different NaOH loadings (0.5 – 5.0 g/L) for Pb(II) removal. Constant conditions:  $C_o = 50$  mg/L,  $m = 0.5$  g/L, pH = 6,  $t = 120$  min,  $T = 27$  °C.

increasing NaOH loadings (from 0 g/L to 1.0 g/L) and decreased at high loadings (> 1.0 g/L). Natural zeolites contain exchangeable alkaline cations in their structural frameworks and permanent negative charges on their surfaces (Zhang et al., 2021). By treating the natural zeolite with NaOH, the silica content was significantly decreased by desilication, and increased the Na<sup>+</sup> content by the formation of hydroxysodalite (Ates and Akgül, 2016). Thus, it promotes the mesopores formation, enhancing the adsorption capacity (Ates, 2018). The formation of mesopores was confirmed by surface area and pore volume analysis. The BET surface area and pore volume of natural zeolite are 67 m<sup>2</sup>/g and 0.18 cm<sup>3</sup>/g, respectively, while the BET surface area and pore volume of natural zeolite after 1.0 g/L NaOH treatment are 26 m<sup>2</sup>/g and 0.14 cm<sup>3</sup>/g, respectively. A decrease in surface area and pore volume after NaOH treatment indicates the formation of mesopores.

However, if the amounts of NaOH treated exceed the optimum point for natural zeolite uptake, it can significantly deform the zeolite structure and reduce the adsorption capacity. Similar findings were reported by Ates (Ates, 2018) for alkaline modification of natural zeolite. For this study, at 1.0 g/L, treatment with NaOH shows good performance of the highest removal (45 %), proving that it is the optimum point for natural zeolite uptake of NaOH. Thus, the selected alkalinized natural zeolite was used for conducting the experimental design, optimization, reusability, and regeneration studies.

Response surface methodology

Table 1 displays the RSM-designed experiments list and the response value (percentage removal) for each sample acquired under the appropriate experimental conditions. The regression analysis was carried out, and the regression function for response in terms of coded components of a statistical model is as follows:

$$Y = -15.1951 + 0.1640X_1 + 18.4420X_2 - 3.1293X_3 + 0.0009X_1X_2 - 0.0003X_1X_3 + 0.016X_2X_3 - 0.0004X_1^2 - 1.5524X_2^2 + 1.3227X_3^2 \tag{3}$$

where Y is the predicted percentage removal of Pb(II), X<sub>1</sub> is initial concentration, X<sub>2</sub> is pH, and X<sub>3</sub> is adsorbent dosage.

Fig. 2 illustrates the actual values of percentage removal of Pb(II) with the predicted values based on Equation (3). The coefficient of determination (R<sup>2</sup>) for percentage removal is 0.9913, implying that 99.13 % of the data variability is elucidated by the model. As reported in the literature, the value should be at least 0.75 or more in order for the empirical model adequately explain most of the variation in essay reading (Jankovic et al., 2021).

Table 1 Experimental design and response surface design outcomes.

No	Manipulated variables						Response
	X <sub>1</sub> (mg/L)	Level	X <sub>2</sub>	Level	X <sub>3</sub> (g/L)	Level	Pb(II) removal (%)
1	50	-1	2	-1	0.50	-1	21.13
2	50	-1	2	-1	5.00	+1	40.85
3	50	-1	10	+1	0.50	-1	22.45
4	50	-1	10	+1	5.00	+1	38.54
5	400	+1	2	-1	0.50	-1	25.88
6	400	+1	2	-1	5.00	+1	40.92
7	400	+1	10	+1	0.50	-1	25.58
8	400	+1	10	+1	5.00	+1	45.14
9	50	-1	6	0	2.75	0	46.50
10	400	+1	6	0	2.75	0	49.36
11	225	0	2	-1	2.75	0	34.29
12	225	0	10	1	2.75	0	33.46
13	225	0	6	0	0.50	-1	55.52
14	225	0	6	0	5.00	+1	78.79
15	225	0	6	0	2.75	0	61.95
16	225	0	6	0	2.75	0	60.37

The analysis of variance (ANOVA) in Table 2 reveals that the F-value of Pb(II) removal is more significant than the calculated F-value (F<sub>0.05</sub> = 2.74). The high F-value proposes that the regression equation can describe a considerable quantity of variation in the response. In short, the model obtained from Equation (3) gives a good prediction at a 5 % significant level.

The t-distribution values and correlated p-values of the modified parameter are shown in a Pareto chart (Fig. 3). The validity of each coefficient was validated by the values of p-value or t-value, whereby the most significant factor can be identified by the smallest p-values and the largest magnitude of t-value. As illustrated in Fig. 3, the most prominent factor is the quadratic pH (X<sub>2</sub><sup>2</sup>), indicated by the smallest p-value (0.000003) and the largest magnitude of t-value (-17.1193) at a

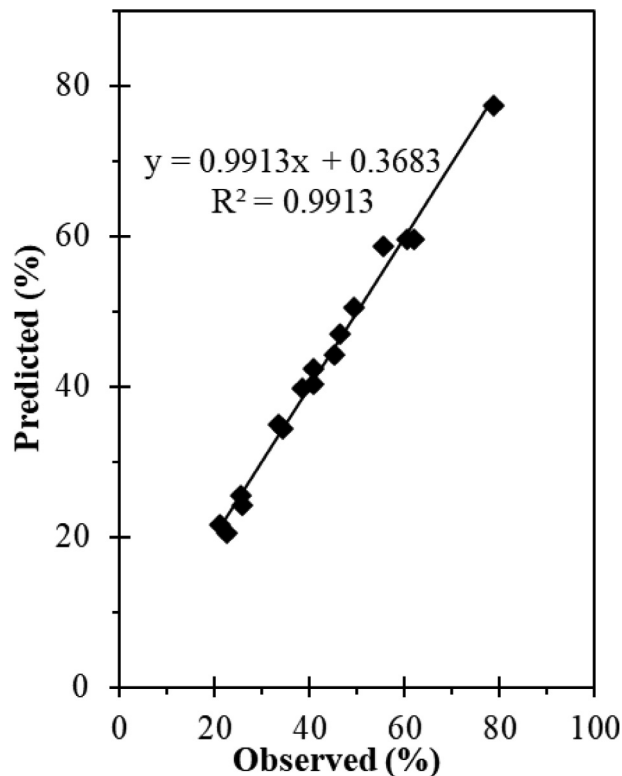
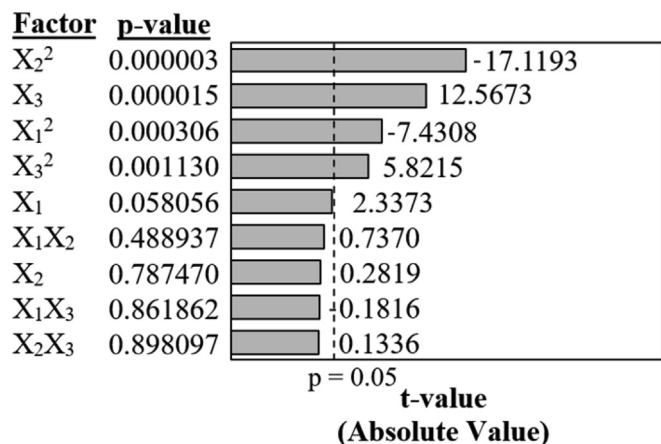


Fig. 2. Parity plot for the observed and predicted percentage removal of Pb(II) using alkaline-treated natural zeolite.

**Table 2**  
ANOVA for percentage removal of Pb(II) using alkaline-treated natural zeolite.

Sources	Sum of squares (SS)	Degree of freedom (d.f)	Mean Square (MS)	F-value	F <sub>0.05</sub>
Regression	3032.05	9	336.90	4.89	> 4.10
Residual	413.28	6	68.88		
Total	3445.34	15			



**Fig. 3.** Pareto chart and p-values for percentage removal of Pb(II) using alkaline-treated natural zeolite.

95 % significant level. On the other hand, linear adsorbent dosage (X<sub>3</sub>), quadratic initial concentration (X<sub>2</sub><sup>2</sup>), and quadratic adsorbent dosage (X<sub>3</sub><sup>2</sup>) are also critical owing to the lower p-value (<0.05). The remaining factors are considered less critical attributable to the higher p-value (>0.05). The most considerable factor attained by X<sub>2</sub><sup>2</sup> can be clarified by the importance of pH because the presence of OH<sup>-</sup> or H<sup>+</sup> affects the surface property, surface charge, and actual state of metal ions (Huang et al., 2020). This is partially attributable to hydrogen ions' intense competition with metal ions (Zhang et al., 2021; Ates and Akgül, 2016).

Response surface plot is a frequent tool for analyzing the correlations between different variables and forecasting the outcome under certain conditions. Fig. 4 shows three response surface plots as the results of varying two parameters while the other parameter was maintained constant. The response surface plot in Fig. 4(A) illustrates the

effects of pH and adsorbent dosage for removing Pb(II). According to the response surface plot analysis, the adsorbent dosage had a more significant influence than pH, which was also interpreted by the Pareto chart (Fig. 3), displaying a larger t-value of adsorbent dosage (12.5673) compared to pH (0.2819). As the amount of adsorbent rises, the Pb(II) removal enhances, passing through a maximum of around 2.75–5 g/L. This behavior may be attributable to an increase in the surface availability of binding sites with an increase in adsorbent dosage (Elboughdiri and Arellano-Garcia, 2020). Moreover, more Pb (II) molecules can be adsorbed due to the presence of mesopores. Meanwhile, the percentage of Pb(II) removal increased with an increase in pH, passing through the maximum pH of 6 and decreasing at higher pH. This condition is explained in terms of ionic strength whereby the Pb(II) molecule exists as Pb<sup>2+</sup>, Pb(OH)<sup>+</sup>, Pb(OH)<sub>2</sub><sup>0</sup> and Pb(OH)<sub>3</sub><sup>-</sup> at different pH conditions, thus affecting the adsorption process (Huang et al., 2020).

Fig. 4(B) depicts the effects of adsorbent dosage and initial Pb(II) concentration on the Pb(II) removal. Significant changes were displayed in the response surface plot, whereby the adsorbent dosage significantly influenced the adsorption process instead of an initial Pb(II) concentration, in line with the larger t-value of adsorbent dosage than the initial Pb(II) concentration (Fig. 3). An increase in the amount of adsorbent dosage significantly increases the Pb(II) adsorption owing to a direct proportion of active sites with adsorbent dosage. Meanwhile, an increase in initial Pb(II) concentrations significantly increases the Pb(II) removal, passing through the optimum and slightly decreasing at elevated values. A slight decrease at higher values of initial Pb(II) concentration due to the limited active site with the superfluous Pb(II) ions (Wang et al., 2020).

Fig. 4(C) portrays the impact of initial Pb(II) concentration and pH on the Pb(II) elimination. As observed, both effects have a high potential increment in the middle of the range (pH = 6, initial Pb(II) concentration = 225 mg/L) and give a high value of percentage removal. A decline in Pb(II) removal at higher pH because the solution became more basic, and precipitation of Pb(II) ions in the solution

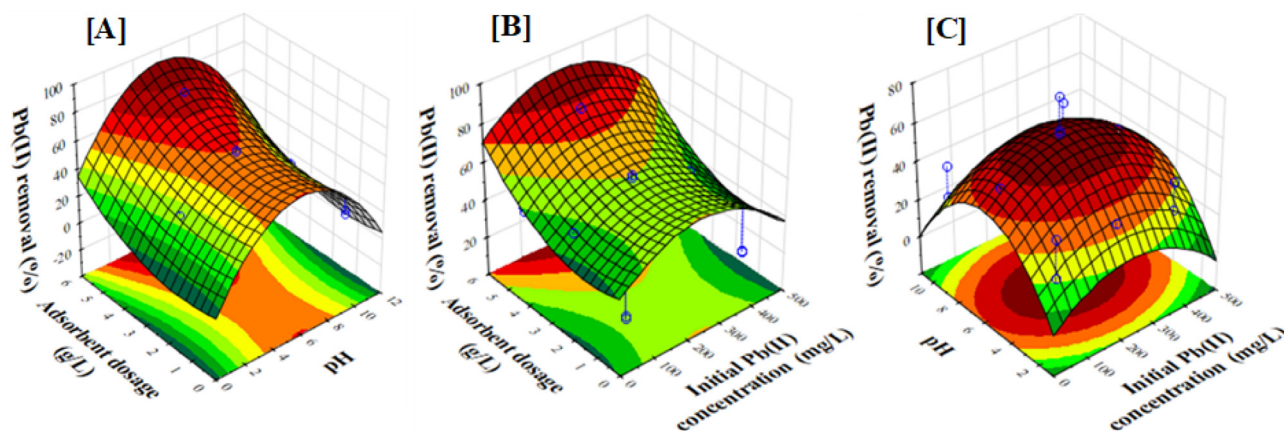


**Fig. 4.** Response surface plot of the combined; (A) pH and adsorbent dosage; (B) Initial Pb concentration and adsorbent dosage; (C) Initial Pb concentration and pH.

(Ates, 2018). Meanwhile, a decline in Pb(II) removal at higher concentrations is attributable to the higher competition of Pb(II) ions for the free accessible binding spaces. The optimum percentage removal of Pb (II) using alkaline-treated natural zeolite was predicted at 58.08 % with the adsorbent dosage of 1.07 g/L, pH of 6, and initial concentration of 240 mg/L. The results of the response surface analysis were validated by conducting an additional experiment with an experimental result of 60.75 % and adsorption capacity of 136.26 mg/g. Therefore, the error gained was 4.60 % and considered acceptable since the error is within the 5 % significance level.

Table S1 compares the adsorption capacity of adsorbent-derived waste materials. As observed, alkaline-treated natural zeolite has the highest adsorption capacity than other adsorbents indicating the high potential of alkaline-treated natural zeolite for the treatment of wastewater containing Pb(II).

*Adsorption kinetics of Pb(II) removal onto Alkaline-Treated natural zeolite*

The kinetic studies were examined by pseudo-first-order and pseudo-second-order kinetic models as described in Equation (4) and Equation (5) (Moussout et al., 2018):

Pseudo-first-order:

$$q_t = q_e(1 - e^{-k_1 t}) \tag{4}$$

Pseudo-second-order:

$$q_t = \frac{k_2 q_e^2 t}{1 + k_2 q_e t} \tag{5}$$

where  $q_e$  (mg/g) and  $q_t$  (mg/g) are the quantity of Pb(II) adsorbed at equilibrium and specific time.  $k_1$  (1/min) and  $k_2$  (g/mg.min) signify pseudo-first-order and pseudo-second-order rate constants.

As illustrated in Fig. S1, the Pb(II) adsorption onto alkaline-treated natural zeolite well fitted the pseudo-second-order model. The kinetic parameter of the pseudo-second-order model shown in Table 3 confirmed this finding, owing to the higher  $R^2$  values (> 0.99) and the insignificant difference between the acquired theoretical values ( $q_{e,cal}$ ) and the experimental values ( $q_{e,exp}$ ). Therefore, it is most likely that the chemisorption process impacted the adsorption of Pb(II) onto alkaline-treated natural zeolite, which was directly related to the reaction rate (Moussout et al., 2018). A similar observation was also reported for the Pb(II) removal onto composite zeolite imidazolate framework@agarose (ZIF-8@AG) (Fu et al., 2022) and potassium ore leaching residue (Xing et al., 2018), in which the experimental adsorption data well fitted with a pseudo-second-order kinetic model.

*Adsorption isotherm of Pb(II) removal onto alkaline-treated natural zeolite*

The adsorption isotherm studies were evaluated by Langmuir, Freundlich, Temkin, and Dubinin-Radushkevich as described in the following linearized forms (Edathil et al., 2018):

Langmuir:

$$\frac{C_e}{q_e} = \frac{1}{q_m K_L} + \frac{C_e}{q_m} \tag{6}$$

Freundlich:

**Table 3**  
Kinetic parameters for Pb(II) adsorption onto alkaline-treated natural zeolite.

Models	Parameters	50 mg/L	100 mg/L	200 mg/L	400 mg/L
Experimental	$q_{e,exp}$ (mg/g)	19.94	42.42	117.11	221.96
	$q_e$ (mg/g)	14.63	13.88	67.34	101.77
Pseudo-first order	$k_1$ ( $\text{min}^{-1}$ )	0.058	0.067	0.062	0.065
	$R^2$	0.977	0.936	0.895	0.850
	$q_e$ (mg/g)	21.14	44.05	120.48	227.27
	$k_2$ ( $\text{min}^{-1}$ )	0.009	0.007	0.003	0.002
Pseudo-second order	$R^2$	0.990	0.996	0.996	0.998

$$\log q_e = \log K_f + \frac{1}{n} \log C_e \tag{7}$$

Temkin:

$$q_e = B \ln A + B \ln C_e \tag{8}$$

Dubinin-Radushkevich:

$$\ln q_e = \ln q_m - K_{DR} \epsilon^2 \tag{9}$$

where  $C_e$  (mg/L) represents the equilibrium Pb(II) concentration, while  $q_e$  (mg/g) and  $q_m$  (mg/g) are the adsorption capacity at equilibrium and maximum.  $K_L$  (L/mg) signifies the Langmuir constant,  $K_f$  ((mg/g)(L/mg)<sup>1/n</sup>) signifies the Freundlich equilibrium constant, meanwhile  $n$  represents an empirical constant. For the Langmuir model, the isotherm shape can be predicted using the dimensionless constant separation factor,  $R_L$ , which can be calculated using  $R_L = 1/(1 + K_L C_o)$ . For the Temkin isotherm model,  $B$  represents the constant, and  $A$  (L/g) signifies the equilibrium binding constant. For the Dubinin-Radushkevich isotherm model,  $K_{DR}$  ( $\text{mol}^2/\text{kJ}^2$ ) represents the constant, and  $\epsilon$  (J/mol) symbolizes the Polanyi potential, which can be calculated using  $\epsilon = RT \ln(1 + 1/C_e)$ , where  $R$  (J/mol·K) is gas constant, and  $T$  (K) is the absolute temperature.

Table 4 shows the computed variables of the studied isotherm models and their linear regression coefficient,  $R^2$ . The most outstanding  $R^2$  value attained by the Langmuir isotherm model (0.999) indicates that Pb(II) adsorption onto alkaline-treated natural zeolite is monolayer adsorption that happens on the homogeneous adsorbent's surface. The Langmuir isotherm was also reported as the excellent isotherm model for Pb(II) removal using a variety of low-cost adsorbents, including FAU-type zeolites derived from coal fly ash (Joseph et al., 2020). The system's  $R_L$  value was 0.919, indicating that Pb(II) adsorption onto alkaline-treated natural zeolite is a desirable system with maximum adsorption of 192.31 mg/g.

*Regeneration and reusability studies*

Fig. 5 illustrates the reusability of alkaline-treated natural zeolite in the adsorption of Pb(II). The reusability analysis was conducted at

**Table 4**  
Isotherm parameters for Pb(II) adsorption onto alkaline-treated natural zeolite.

Isotherm	Parameters	Value
Langmuir	$q_m$ (mg/g)	192.31
	$K_L$ (L/mg)	0.003
	$R^2$	0.919
	$R_L$	0.999
Freundlich	$n$	0.719
	$K_f$ (mg/g)(L/mg) <sup>1/n</sup>	0.172
	$R^2$	0.999
Temkin	$B$ (J/mol)	117.4
	$A$ (L/g)	0.032
	$R^2$	0.850
Dubinin-Radushkevich	$q_m$ (mg/g)	120.12
	$K_{ad}$ ( $10^4$ )	3
	$R^2$	0.720

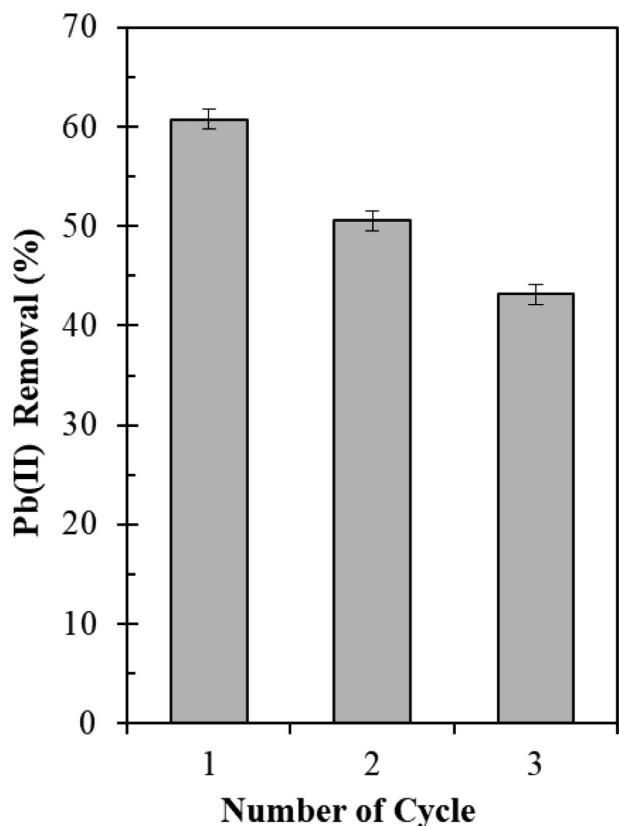


Fig. 5. The regeneration and reusability experiment of Pb(II) removal using alkaline-treated natural zeolite. Conditions:  $m = 1.07$  g/L,  $\text{pH} = 6$ ,  $C_o = 240$ -mg/L,  $T = 27$  °C.

$C_o = 240$  mg/L,  $\text{pH} = 6$ ,  $m = 1.07$  g/L, and  $T = 27$  °C for 120 min each cycle. The regeneration process was performed after each cycle using phosphoric acid. As illustrated, the alkaline-treated natural zeolite can be utilized for up to 3 cycles with a minor reduction in adsorption performance (17.6 %), indicating the good potential of alkaline-treated natural zeolite in multiple adsorption cycles.

Characterization

The SEM images of alkaline-treated natural zeolite before and after Pb(II) adsorption are depicted in Fig. 6. The SEM alkaline-treated natural zeolite before adsorption (Fig. 6(A)) showed a rough and porosity texture, indicating its suitability for adsorption. After Pb(II) adsorption experiment, the pores of alkaline-treated natural zeolite were occupied

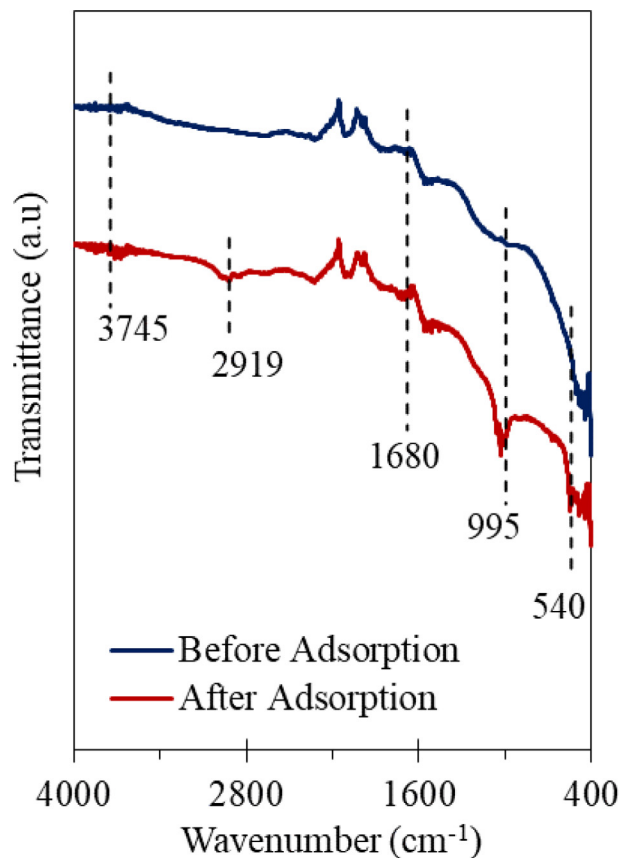


Fig. 7. FTIR spectra before and after adsorption of alkaline-treated natural zeolite.

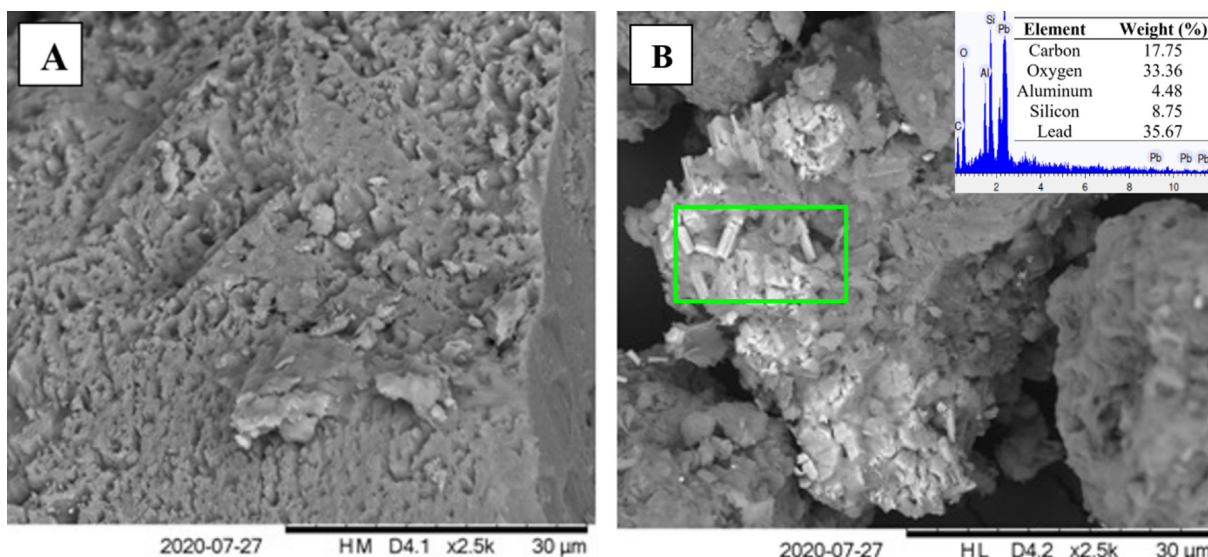


Fig. 6. SEM images of alkaline-treated natural zeolite under magnification of  $2500 \times$  (A) before adsorption; (B) after adsorption.

and attached with tiny white particles (Fig. 6(B)). The tiny white particles implied the adsorption of Pb(II) onto the alkaline-treated natural zeolite. From the EDX analysis (inset of Fig. 6(B)), it was clearly showed the elemental composition of Pb(II) has the highest weight percentage, followed by O, C, Si, and Al. Thus, demonstrating successful adsorption of Pb(II) on the surface of alkaline-treated natural zeolite. The spent adsorbent's surface structure is also reported in the literature (Wang and Zhang, 2021).

The existence of Pb(II) on the surface of spent alkaline-treated natural zeolite was further confirmed by the FTIR analysis revealed in Fig. 7. Before adsorption, the FTIR spectra of alkaline-treated natural zeolite showed four prominent peaks at  $3745\text{ cm}^{-1}$ ,  $1680\text{ cm}^{-1}$ ,  $995\text{ cm}^{-1}$ , and  $540\text{ cm}^{-1}$ , assigned to the terminal silanol (Si-OH) groups, deformation vibration of hydroxyl (-OH) groups, stretching of asymmetric T-O bonds (T = Si or Al), and vibration of T-O-T, respectively (Lim et al., 2021). After adsorption, these peaks remain appeared with the presence of a new peak observed at  $2919\text{ cm}^{-1}$ . The peak at  $2919\text{ cm}^{-1}$  may be attributed to the existence of Pb(II) on the surface of alkaline-treated natural zeolite after the adsorption process.

## Conclusions

The adsorption study by alkaline-treated natural zeolite revealed that the optimal NaOH loading is 1 g/L, presented by the highest Pb(II) removal. This finding is due to an improvement in the mesoporosity of the natural zeolite, which enhances its adsorption capacity. The optimum alkaline-treated natural zeolite was successfully prepared, characterized, and applied in Pb(II) removal by RSM. The optimization by RSM discovered that the optimum condition was attained at an adsorbent mass of 1.07 g/L, pH of 6, 240 mg/L of initial concentration of Pb(II) with a percentage removal of 60.75 %, and adsorption capacity of 136.26 mg/g. In addition, this study also successfully developed the mathematical model of Pb(II) removal with a good prediction at a 5 % significant level. The regeneration and reusability experiment showed that the alkaline-treated natural zeolite could be utilized for up to 3 cycles with minor performance removal. Therefore, this study proved the positive role of alkali treatment in improving adsorbent's properties and activity. Additionally, this study evidenced the great potential of copious natural earth resources as a source of alternative low-cost adsorbents for the treatment of wastewater.

## Data availability

No data was used for the research described in the article.

## Declaration of Competing Interest

The authors declare that they have no known competing financial interests or personal relationships that could have appeared to influence the work reported in this paper.

## Acknowledgment

The financial assistance provided by Universiti Malaysia Pahang via International Publication Grant (RDU203303) is acknowledged.

## Author statement

N.A.S. El-Arish executed the experimental procedure and wrote the original manuscript draft. R.S.R. Mohd Zaki and S.N. Miskan contributed to interpreting the results and the final manuscript. H.D. Setiabudi conceptualized the research idea, supervised the research, and contributed to the final manuscript. N.F. Jaafar verified the experimental procedure and contributed to the final manuscript.

## Appendix A. Supplementary data

Supplementary data to this article can be found online at <https://doi.org/10.1016/j.totert.2022.100015>.

## References

- Ates, A., 2018. Effect of alkali-treatment on the characteristics of natural zeolites with different compositions. *J. Colloid Interface Sci.* 523, 266–281. <https://doi.org/10.1016/J.JCIS.2018.03.115>.
- Ates, A., Akgül, G., 2016. Modification of natural zeolite with NaOH for removal of manganese in drinking water. *Powder Technol.* 287, 285–291. <https://doi.org/10.1016/j.powtec.2015.10.021>.
- Din, M.I., Khalid, R., Najeeb, J., Hussain, Z., 2021. Fundamentals and photocatalysis of methylene blue dye using various nanocatalytic assemblies- a critical review. *J. Clean. Prod.* 298, <https://doi.org/10.1016/J.JCLEPRO.2021.126567> 126567.
- Edathil, A.A., Shittu, I., Hisham Zain, J., Banat, F., Haija, M.A., 2018. Novel magnetic coffee waste nanocomposite as effective bioadsorbent for Pb(II) removal from aqueous solutions. *J. Environ. Chem. Eng.* 6, 2390–2400. <https://doi.org/10.1016/J.JECE.2018.03.041>.
- Elboughdiri, N., Arellano-Garcia, H., 2020. The use of natural zeolite to remove heavy metals Cu (II), Pb (II) and Cd (II), from industrial wastewater. *Cogent Eng.* 7 (1), 1782623.
- Fu, Q., Zhou, S., Wu, P., Hu, J., Lou, J., Du, B., Mo, C., Yan, W., Luo, J., 2022. Regenerable zeolitic imidazolate frameworks@agarose (ZIF-8@AG) composite for highly efficient adsorption of Pb(II) from water. *J. Solid State Chem.* 307, 122823.
- GilPavas, E., Dobrosz-Gómez, I., Gómez-García, M.Á., 2020. Efficient treatment for textile wastewater through sequential electrocoagulation, electrochemical oxidation and adsorption processes: Optimization and toxicity assessment. *J. Electroanal. Chem.* 878, <https://doi.org/10.1016/J.JELECHEM.2020.114578> 114578.
- Hargreaves, A.J., Vale, P., Whelan, J., Alibardi, L., Constantino, C., Dotro, G., Cartmell, E., Campo, P., 2018. Coagulation-flocculation process with metal salts, synthetic polymers and biopolymers for the removal of trace metals (Cu, Pb, Ni, Zn) from municipal wastewater. *Clean Technol. Environ. Policy* 20 (2), 393–402.
- Hasan, R., Setiabudi, H.D., 2019. Removal of Pb(II) from aqueous solution using KCC-1: optimization by response surface methodology (RSM). *J. King Saud Univ. Sci.* 31, 1182–1188. <https://doi.org/10.1016/J.JKSUS.2018.10.005>.
- Hasan, R., Chong, C.C., Bukhari, S.N., Jusoh, R., Setiabudi, H.D., 2019. Effective removal of Pb(II) by low-cost fibrous silica KCC-1 synthesized from silica-rich rice husk ash. *J. Ind. Eng. Cem.* 75, 262–270. <https://doi.org/10.1016/J.JIEC.2019.03.034>.
- Huang, R., Lin, Q., Zhong, Q., Zhang, X., Wen, X., Luo, H., 2020. Removal of Cd(II) and Pb(II) from aqueous solution by modified attapulgite clay. *Arab. J. Chem.* 13, 4994–5008. <https://doi.org/10.1016/J.ARABJC.2020.01.022>.
- Inglezakis, V.J., Fyrrillas, M.M., Stylianou, M.A., 2018. Two-phase homogeneous diffusion model for the fixed bed sorption of heavy metals on natural zeolites. *Microporous Mesoporous Mater.* 266, 164–176. <https://doi.org/10.1016/J.MICROMESO.2018.02.045>.
- Jankovic, A., Chaudhary, G., Goia, F., 2021. Designing the design of experiments (DOE) – An investigation on the influence of different factorial designs on the characterization of complex systems. *Energy Build.* 250, <https://doi.org/10.1016/J.ENBUILD.2021.111298> 111298.
- Joseph, I.V., Tosheva, L., Doyle, A.M., 2020. Simultaneous removal of Cd(II), Co(II), Cu (II), Pb(II), and Zn(II) ions from aqueous solutions via adsorption on FAU-type zeolites prepared from coal fly ash. *J. Environ. Chem. Eng.* 8 (4), 103895.
- Lim, W.R., Lee, C.H., Hamm, S.Y., 2021. Synthesis and characteristics of Na-A zeolite from natural kaolin in Korea. *Mater. Chem. Phys.* 261, <https://doi.org/10.1016/J.MATCHEMPHYS.2021.124230> 124230.
- Morante-Carballo, F., Montalván-Burbano, N., Carrión-Mero, P., Jácome-Francis, K., 2021. Worldwide research analysis on natural zeolites as environmental remediation materials. *Sustainability* 13, 6378. <https://doi.org/10.3390/SU13116378>.
- Moussout, H., Ahlafi, H., Aazza, M., Maghat, H., 2018. Critical of linear and nonlinear equations of pseudo-first order and pseudo-second order kinetic models. *Karbala Int. J. Mod. Sci.* 4, 244–254. <https://doi.org/10.1016/J.KIJOMS.2018.04.001>.
- Ohlbaum, M., Wadgaonkar, S.L., van Bruggen, J.J.A., Nanchariaiah, Y.V., Lens, P.N.L., 2018. Lens, Phytoremediation of seleniferous soil leachate using the aquatic plants Lemna minor and Egeria densa. *Ecol. Eng.* 120, 321–328.
- Roy Choudhury, P., Majumdar, S., Sarkar, S., Kundu, B., Sahoo, G.C., 2019. Performance investigation of Pb(II) removal by synthesized hydroxyapatite based ceramic ultrafiltration membrane: Bench scale study. *Chem. Eng. J.* 355, 510–519. <https://doi.org/10.1016/J.CEJ.2018.07.155>.
- Shang, E., Li, Y., Niu, J., Li, S., Zhang, G., Wang, X., 2018. Photocatalytic degradation of perfluorooctanoic acid over Pb-BiFeO<sub>3</sub>/rGO catalyst: kinetics and mechanism. *Chemosphere* 211, 34–43. <https://doi.org/10.1016/J.CHEMOSPHERE.2018.07.130>.
- Skibsted, G., Ottosen, L.M., Elektorowicz, M., Jensen, P.E., 2018. Effect of long-term electrodialytic soil remediation on Pb removal and soil weathering. *J. Hazard. Mater.* 358, 459–466. <https://doi.org/10.1016/J.JHAZMAT.2018.05.033>.
- Teong, C.Q., Setiabudi, H.D., El-Arish, N.A.S., Bahari, M.B., Teh, L.P., 2019. Vatica rassak wood waste-derived activated carbon for effective Pb(II) adsorption: Kinetic, isotherm and reusability studies. *Mater Today Proc* 42, 165–171. <https://doi.org/10.1016/j.matpr.2020.11.270>.

- Vardhan, K.H., Kumar, P.S., Panda, R.C., 2019. A review on heavy metal pollution, toxicity and remedial measures: current trends and future perspectives. *J. Mol. Liq.* 290, <https://doi.org/10.1016/J.MOLLIQ.2019.111197> 111197.
- Wang, S., Liu, Y., Lü, Q.F., Zhuang, H., 2020. Facile preparation of biosurfactant-functionalized Ti<sub>2</sub>CTX MXene nanosheets with an enhanced adsorption performance for Pb(II) ions. *J. Mol. Liq.* 297, <https://doi.org/10.1016/J.MOLLIQ.2019.111810> 111810.
- Wang, J., Zhang, W., 2021. Evaluating the adsorption of Shanghai silty clay to Cd(II), Pb(II), As(V), and Cr(VI): kinetic, equilibrium, and thermodynamic studies. *Environ. Monit. Assess.* 193, 1–23. <https://doi.org/10.1007/S10661-021-08904-7>.
- Wu, Y., Tian, F., Liu, J., Song, D., Jia, C., Chen, Y., 2012. Enhanced catalytic isomerization of  $\alpha$ -pinene over mesoporous zeolite beta of low Si/Al ratio by NaOH treatment". *Microporous Mesoporous Mater.* 162, 168–174. <https://doi.org/10.1016/j.micromeso.2012.06.027>.
- Wu, J., Wang, T., Wang, J., Zhang, Y., Pan, W.P., 2021. A novel modified method for the efficient removal of Pb and Cd from wastewater by biochar: Enhanced the ion exchange and precipitation capacity. *Sci. Total Environ.* 754, <https://doi.org/10.1016/J.SCITOTENV.2020.142150> 142150.
- Xing, P., Wang, C., Ma, B., Chen, Y., 2018. Removal of Pb(II) from aqueous solution using a new zeolite-type adsorbent: potassium ore leaching residue. *J. Environ. Chem. Eng.* 6, 7138–7143. <https://doi.org/10.1016/J.JECE.2018.11.003>.
- Yang, R., Cao, Q., Liang, Y., Hong, S., Xia, C., Wu, Y., Li, J., Cai, L., Sonne, C., Le, Q.V., Lam, S.S., 2020. High capacity oil absorbent wood prepared through eco-friendly deep eutectic solvent delignification. *Chem. Eng. J.* 401, 126150.
- Zhang, X., Song, Z., Dou, Y., Xue, Y., Ji, Y., Tang, Y., Hu, M., 2021. Removal difference of Cr(VI) by modified zeolites coated with MgAl and ZnAl-layered double hydroxides: efficiency, factors and mechanism. *Colloids Surf A Physicochem. Eng. Asp.* 621, 126583.